

Radiobiological features of the anti-cancer strategies involving synchrotron X-rays

Zuzana Bencokova,^a Jacques Balosso^{a,b} and Nicolas Foray^{a*}

Received 16 March 2007

Accepted 13 September 2007

^aINSERM U647, ID17, European Synchrotron Research Facility, 38043 Grenoble, France, and^bDépartement de Cancérologie et d'Hématologie, CHU Michallon, Grenoble, France.

E-mail: foray@esrf.fr

Synchrotrons are opening new paths in innovative anti-cancer radiotherapy strategies. Indeed, the fluence of X-rays induced by synchrotrons is so high (10^6 times higher than standard medical irradiators) that it enables the production of X-ray beams tunable in energy (monochromatic beams) and in size (micrometric beams). Monochromatic synchrotron X-ray beams theoretically permit photoactivate high-Z elements to be introduced in or close to tumours in order to increase the yield of damage by enhanced energy photoabsorption. This is notably the case of attempts with iodinated contrast agents used in tumour imaging (the computed tomography therapy approach) and with platinated agents used in chemotherapy (the PAT-Plat approach). Micrometric synchrotron X-ray beams theoretically permit very high radiation doses to accumulate in tumours by using arrays of parallel microplanar beams that spare the surrounding tissues (the microbeam radiation therapy approach). These anti-cancer applications of synchrotron radiation have been developed at the European Synchrotron Radiation Facility to be applied to glioma, one of the tumour tissues most refractory to standard treatments. In the present paper the molecular and cellular mechanisms involved in these three approaches are reviewed, in the context of recent advances in radiobiology. Furthermore, by considering the unavoidable biases, an attempt to propose a comparison of the different results obtained in preclinical trials dealing with rats bearing tumours is given.

© 2008 International Union of Crystallography
Printed in Singapore – all rights reserved

Keywords: DNA repair; CT therapy; PAT; MRT.

1. Introduction

To date, the great majority of tumours are treated by surgery and/or by treatments combining chemotherapy and radiotherapy. With regard to radiotherapy, standard medical irradiators generally provide high-energy photons that are facilitating the treatment of deep-seated tumours owing to their high penetration in matter. However, high-energy photons do not necessarily produce optimal biological effects and their development has not fully eliminated the crucial problem of deleterious effects in surrounding normal tissues.

Recently, synchrotrons have opened a new path in innovative radiotherapy strategies. Indeed, the fluence of X-rays induced by synchrotrons is so high (10^6 times higher than standard medical irradiators) that it enables the production of X-ray beams tunable in energy (monochromatic beams) and in size (micrometric beams). Since the 1990s, a considerable amount of data have been accumulated in the field of medical applications of synchrotron radiation, notably to treat gliomas. In parallel, since radiation and drugs *per se* are often efficient

enough to kill tumours, the general recent tendency in the development of new anti-cancer strategies is to secure the clinical transfer by a better knowledge of the molecular, cellular and tissular mechanisms specifically induced in normal tissues. Hence, throughout this review we have endeavoured to understand, evaluate and compare the radiobiological features of the anti-cancer treatments involving synchrotron radiation.

1.1. Interest of monochromatic and micrometric synchrotron X-rays

Monochromatic synchrotron X-ray beams theoretically permit the enhancement of photoelectric, Compton and/or Auger effects in high-Z elements that are contained in drugs injected during irradiation. This so-called photoactivation of high-Z elements aims therefore to increase the yield of damage by enhancing energy absorption (Corde *et al.*, 2003; Biston *et al.*, 2004; Adam *et al.*, 2003). The X-ray energies of photoactivation that have been used generally correspond to

either the absorption edge (*K*- or *L*-edge) or to maximizing the relative X-ray absorption of the high-*Z* element in water. Two variant photoactivation therapies are developed, differing by the photoactivable drugs that are used.

(i) Most imaging contrast agents that are employed in standard radiodiagnostics [computed tomography (CT) imaging, urography, angiography *etc.*] contain iodine atoms. By irradiating iodine-loaded tumours at the appropriate energy, an enhanced energy absorption may contribute to increase the therapeutic index. This approach was initially called CT therapy and performed with polychromatic irradiation (Norman *et al.*, 1978). It has been pursued with monochromatic synchrotron radiation (Adam *et al.*, 2003, 2006). More recently, the possibility to photoactivate contrast agents containing gadolinium atoms used in nuclear magnetic resonance imaging has been investigated (De Stasio *et al.*, 2006).

(ii) Some chemotherapeutic drugs that are used extensively in standard cancer treatments contain high-*Z* elements. This is notably the case of platinated agents such as cisplatin and carboplatin (Cepeda *et al.*, 2007). By irradiating platinum-loaded tumours at the appropriate energy, an enhanced energy absorption is therefore expected to be added to the effect of the chemotherapeutic drug alone (Corde *et al.*, 2003; Biston *et al.*, 2004).

Micrometric synchrotron X-ray beams theoretically permit the accumulation of very high radiation doses into tumours in a single fraction by using arrays of microplanar beams of X-rays (Laissie *et al.*, 1998; Dilmanian *et al.*, 2005). This technique has been called microbeam radiation therapy (MRT). The advantages of microbeams are their sparing effect on normal tissues and their preferential damage to tumours, even when administrated in a single direction (Dilmanian *et al.*, 2005). The MRT approach is also based on the assumption that microscopic thin planar slices of synchrotron-generated X-rays permit the rapid regeneration of normal microvessels. Conversely, the accumulation of dose owing to the overlap of microbeams was hypothesized to prevent the recovery of tumour vasculature (Dilmanian *et al.*, 2006; Miura *et al.*, 2006; Smilowitz *et al.*, 2006).

1.2. Recent advances in radiobiology

In parallel to these recent developments, our understanding in biological effects of ionizing radiation has considerably progressed these last years, notably in the fields of DNA damage repair and stress signalling (Khanna & Jackson, 2001; Rothkamm & Lobrich, 2003; Joubert & Foray, 2006). In particular, four major features of radiobiology are revolutionizing the evaluation of anti-cancer approaches and must therefore be taken into account for the medical applications of synchrotron radiation.

(i) After irradiation of living matter, physical, chemical, biochemical and biological events are intimately mixed in a complex cascade of events. Hence, clinical response is the integrated result of molecular, cellular and tissue events whose time scale of occurrence is clearly different. On one hand,

theoretical simulations of the radiation dose distribution are useful for predicting the amount of DNA damage induced in the first seconds of irradiation. Conversely, these simulations of physico-chemical events are obviously unable to predict the kinetics of DNA damage repair that occurs in the first hours of irradiation and that is correlated to survival. On the other hand, preclinical trials with animal models, taken separately, are also insufficient to provide mechanistic insights in early events. Hence, the evaluation of an anti-cancer approach requires not only quantitative data about its therapeutic efficacy against tumours but also a better knowledge of all the molecular, cellular and tissue events that it generates (Joubert & Foray, 2006).

(ii) Most of the anti-cancer strategies are based on the concept of depositing dose more efficiently into tumours. However, to date, there is evidence that the amount of induced DNA damage is not predictive of the final response of tumours to radiation. Conversely, the amount of unrepaired DNA damage appears to be a more relevant parameter for predicting tumour killing (Steel, 2002). Furthermore, some tumours possess an impressive capacity for repairing DNA and patients may succumb to dose-dependent side effects before tumour growth is influenced by the treatment (Chavaudra *et al.*, 2004; Joubert & Foray, 2006). Hence, to date, any anti-cancer approach should be evaluated more preferentially by the prediction of its effects on normal tissues rather than its efficacy in killing tumours.

(iii) This last point is of importance since the absorbed radiation dose appears to date to be an insufficient notion for describing the effects of radiation at the molecular level. Indeed, it must be stressed that the absorbed radiation dose was historically defined as a macroscopic value (J kg^{-1}) and is not relevant for describing the distribution of energy micro-depositions in cell nuclei (Goodhead *et al.*, 1981). Furthermore, new advances in bystander and delayed radiation-induced effects show that these effects contribute to the formation of DNA damage that are not considered by the radiation dose defined in Gy (Mothersill & Seymour, 2004).

(iv) Ionizing radiation and chemotherapy drugs induce a large spectrum of DNA damage differing in their biochemical type, their induction rate, and the way by which they are repaired. Radiotherapy notably produces DNA double-strand breaks that are generally repaired by a so-called non-homologous end-joining (NHEJ) pathway that roughly consists of ligating broken DNA ends (Jeggo & Lobrich, 2006). Chemotherapy-induced DNA damage is not necessarily DNA breaks but more frequently DNA crosslinks that activate repair pathways consisting of excising such DNA damage and replacing the missing DNA strand through a complex cascade of events with strand exchange and polymerization (Dudas & Chovanec, 2004). The interplay of the different DNA repair pathways occurring when radiotherapy and chemotherapy are concomitant can generate antagonistic or synergistic effects on DNA damage induction and repair (Turchi *et al.*, 1997). Furthermore, combined treatments increase the impact of the genetic status of the patients that may influence their clinical response to radiotherapy and to chemotherapy (Joubert &

Foray, 2006). Hence, the genetic status of patients and that of their tumours need to be taken into account in asserting their response to radiochemotherapy to not only enhance the therapeutic effect against the tumour but also to prevent acute reactions in normal tissues.

It appears therefore crucial to consider to date the potential impact of innovative anti-cancer approaches, whether involving synchrotron X-rays or not, throughout an integrative and transversal approach of physical, biochemical and biological analysis to better take into account individual specificities. In the following chapters we have reviewed the three major anti-cancer strategies involving synchrotron X-rays by considering their specific radiobiological features and the biological assumptions on which they are based.

2. Applications of monochromatic synchrotron X-rays

2.1. Use of contrast agents: CT therapy

2.1.1. Main principles and first results. When tumour imaging is performed by using X-ray CT scanners, iodinated contrast agents (ICAs) are injected into the blood before and/or during the radiodiagnostic sessions in order to visualize the tumour through the enhanced X-ray photoabsorption of iodine. Historically, the first medical application of photoactivation has to be attributed to Norman's group. In the 1970s, Norman and colleagues observed chromosomal aberrations and micronuclei in circulating lymphocytes of nine patients submitted to urography and cardiac angiography involving ICAs (Adams *et al.*, 1977; Norman *et al.*, 1978). In these radiodiagnostic sessions a dose of 2 cGy was delivered by a standard polychromatic X-ray tube (65–75 kVp, 1.3 mA). These cytogenetic findings were similar to those assessed *in vitro* without ICAs at 20 and 30 cGy. Norman *et al.* hypothesized therefore that such aberrations resulted from a local excess of radiation dose, attributed to an enhanced photoelectric effect owing to the energy absorption by iodine atoms contained in ICAs. Their conclusions were confirmed with a meta-analysis of ten clinical studies using ICAs during angiography or excretory urography (Norman *et al.*, 2001). Norman and colleagues proposed to 'exploit' these chromosome-damaging effects by applying them to brain tumours while (i) loading the tumour with ICAs by intravenous injection, (ii) imaging the tumour with a modified X-ray CT system (imaging over 360° with three non-coplanar axes) and computing the tumour position; and (iii) treating the tumour with the same irradiation set-up by using the computed attenuation data obtained during imaging and by photoactivating ICAs accumulated in the tumour vasculature (Fig. 1).

Hence, the CT therapy approach combined optimized tumour targeting (stereotaxic tomographic irradiation) and differential biological effects owing to the photoactivation of ICAs present in the tumour during irradiation. X-rays used in CT therapy were initially those used in radiodiagnostic (*i.e.* high voltage lower than 150 kV, corresponding to a mean energy of roughly 100 keV). This technique presented the

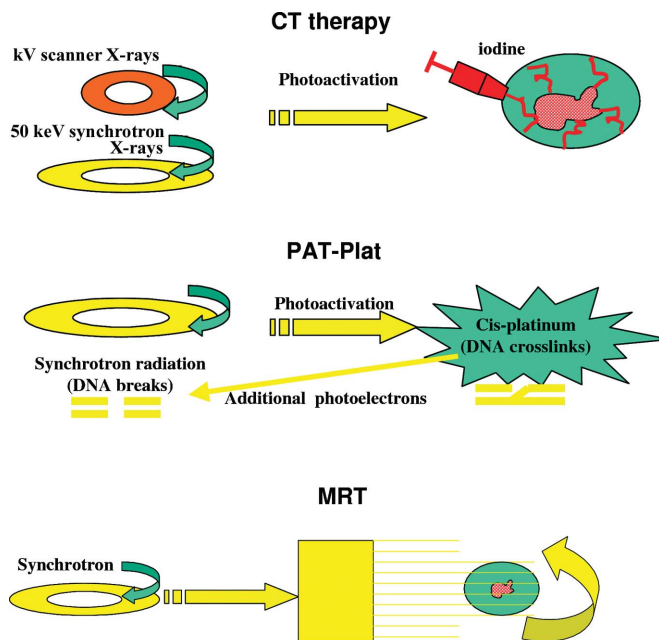


Figure 1 Schematic illustration of the three major anti-cancer modalities involving synchrotron radiation. CT therapy is based on the photoactivation of iodine contained in iodinated contrast agent that has been injected intravenously into the tumour before irradiation. PAT-Plat is based on the photoactivation of platinum contained in the platinumated chemotherapeutic drugs that has been injected intravenously into the tumour before irradiation. MRT is a grid radiotherapy that delivers a very high dose into the tumour *via* thin X-ray microbeams that spare normal tissues.

considerable advantage of reducing patient displacement during treatment (Table 1). Although such a strategy did not overcome the problem of chromosomal aberrations in normal tissues (observations on which this technique was based), it was applied to animals with limited success (Iwamoto *et al.*, 1993, 1987; Santos Mello *et al.*, 1983; Norman *et al.*, 1997) and to humans in a unique clinical trial combined with standard radiotherapy sessions (Rose *et al.*, 1999). To our knowledge, since 1990, no other clinical trial has been performed using this approach.

Subsequently, new preclinical trials were performed at the European Synchrotron Radiation Facility (ESRF) by applying monochromatic X-rays to brain tumours of rats that were injected with ICAs either intravenously or *via* the carotid (Adam *et al.*, 2006). It is noteworthy that ICAs were injected concomitantly with an infusion of hyperosmotic blood-brain barrier opener, the mannitol, which does not make the evaluation of the effect of ICA alone easy. Three X-ray doses (5, 15, 25 Gy) and two iodine injection modalities were tested. The maximal median survival time obtained with iodine was 71 days (15 Gy; intracarotid injection) while the rats treated with 25 Gy without iodine showed a median survival time of 145 days (Adam *et al.*, 2006).

2.1.2. Radiobiological analysis. In the synchrotron experiments the X-ray energy used was 50 keV, corresponding to the maximal relative X-ray absorption of an iodine solution in water, whereas the *K*-edge of iodine is 33.17 keV, which corresponds to the local maximum photoelectric cross section.

Table 1

Principle, advantages and inconveniences of each anti-cancer strategy using synchrotron radiation.

Method	Principle	Hypothesis	Advantages	Inconveniences
Microbeam radiation therapy (MRT)	High-dose radiotherapy in one or several directions by multiple parallel planar microbeams	Physical dose excess will contribute to kill tumour	Tissue necrosis prevention by repopulation of normal tissues from cells in valleys	Patient displacements; residual dose in valleys; bystander effects still not known; numerous irradiation parameters (dose, beam size, valley size <i>etc.</i>)
Photoactivation of iodinated contrast agents (CT therapy)	Stereotactic radiotherapy by enhancement of photoelectric effect in tumour <i>via</i> ICAs	Physical dose excess will contribute to kill tumour	Concomitant tumour imaging and radiotherapy; intravenous application	Extravascular diffusion; extranuclear photoactivation; toxicity of radiolysis products
Photoactivation of platinated compounds (PAT-Plat)	Stereotactic radiotherapy by enhancement of photoelectric effect in tumour <i>via</i> platinated chemotherapeutic compounds	Physical dose excess will contribute to kill tumour	Intratumoral accumulation; intranuclear photoactivation; direct DNA targeting; synergic effect of radio- and chemotherapy are enhanced by photoactivation	Intracranial (intra-tumoral) injection

The choice of the energy of 50 keV was justified by the authors by the evaluation of clonogenic survival after irradiating cells at different X-ray energies in the presence of ICAs (Corde *et al.*, 2004). In the context of theoretical studies of CT therapy, Monte Carlo simulations confirmed also that an excess of dose should be actually delivered into the tumour, suggesting an enhancement of the therapeutic index with CT therapy (Boudou *et al.*, 2005). Further, other iodinated compounds [*e.g.* iododeoxyuridine (IudR), iodides *etc.*] may be used in the frame of CT therapy (Fairchild *et al.*, 1982). However, intrinsic biological effects of ICAs, IudR and iodides are very different. For example, IudR alone induces synchronization in the S phase and iodides inhibit DNA repair. Such particularities raise two questions: (i) how are the biological effects of photoactivable molecules that contain a given high-*Z* element predicted? (ii) what level of description is needed in a simulation code to predict capabilities for synergistic effects?

ICAs are complex molecules that do not enter into cells and remain bound to the external cell membrane. Conversely, IudR, a base analog molecule, or iodides like NaI or KI are able to cross the cell membrane and target DNA (Joubert *et al.*, 2005). Some ¹²⁵I iodide forms or IudR molecules are commonly used in targeted therapy based on internal contamination. Conversely, therapeutic use of ICAs is limited (Fairchild, 1987; Mitchell *et al.*, 1989; Laster *et al.*, 1993; Kassis & Adelstein, 1996). To investigate further the relative failure of CT therapy, investigations were performed *in vitro*, notably in the DNA damage repair field. Irradiation of cells at 50 keV in the presence of ICAs does not produce any significant excess of the amount of DNA damage as it would be expected if an excess of dose was delivered to the tumour (Joubert *et al.*, 2005). However, the toxicity (unrepaired breaks, micronuclei) observed in treated cells suggested an impact upon DNA repair pathways. Interestingly, irradiation of ICAs at 50 keV triggers the optimized radiolysis of ICAs molecules and results in their chemical decomposition by liberating iodide ions. Iodide ions are able to cross membranes and to bind to DNA.

Once onto DNA, iodides are capable of inhibiting DNA repair processes by a steric prevention of accessibility of repair proteins (Joubert *et al.*, 2005). Hence, the irradiation of cells in the presence of ICAs may result in an inhibition of DNA repair owing to the extracellular liberation of iodide ions rather than an extra-production of DNA damage. Unfortunately, photoactivation-induced iodides may diffuse through vasculature into normal tissues and also prevent DNA repair of normal cells that were irradiated during treatment (Joubert *et al.*, 2005). The cellular consequences of such treatment are logically micronuclei and apoptotic bodies that contribute to increase toxicity through the production of chromosomal aberrations in surrounding normal tissues (Joubert *et al.*, 2005). Hence, this molecular model may provide a relevant explanation of the previous findings of Norman's group described above and the relative failure of the monochromatic CT therapy in increasing more significantly the survival of rats bearing tumours than X-ray treatment alone (Adam *et al.*, 2003, 2006). Hence, particular care must be taken in the application of techniques based on the presence of chromosomal aberrations already observed in surrounding normal tissues. A strict evaluation of the toxicity eventually induced in normal tissues is therefore required before considering the efficiency of the treatment to the tumour. Lastly, further investigations in the early events occurring after a photoactivation therapy is also needed to better justify the choice of the X-ray energy applied. Additional CT therapy experiments may be therefore useful to better understand the basic mechanisms of X-ray photoactivation.

2.2. Photoactivation of platinated agents (PAT-Plat)

2.2.1. Main principles and first results. CT therapy opened the wide field of photoactivation of other pharmacological compounds containing high-*Z* elements. Platinum-containing drugs like cisplatin, carboplatin and oxaliplatin appeared early to be the best candidates for anti-cancer strategies involving

photoactivation (PAT) since they are already extensively used in various chemotherapy and chemoradiotherapy treatments. Such drugs bind to DNA by forming DNA adducts and target preferentially proliferating cells in S-G2/M phases, and therefore preferentially tumours (Cepeda *et al.*, 2007; Rabik & Dolan, 2007). These drugs contain platinum atoms that are theoretically photoactivable at 78.4 keV, corresponding to the *K*-edge of platinum. PAT of cisplatin (PAT-Plat) has been particularly developed at ESRF. Recently, PAT-Plat provided by synchrotron X-rays was applied to rats bearing radio-resistant gliomas. After a cisplatin intratumoral injection, 15 Gy X-rays were delivered by synchrotron radiation into a tumour just above the Pt *K*-edge (78.8 keV). This treatment resulted in the cure of 33% rats and still provides to date the most protracted survival of rats bearing F98 glioma models (Biston *et al.*, 2004). More recently, the use of carboplatin, a platinated compound that is less neurotoxic than cisplatin, permitted to increase rat survival up to 44% (Biston *et al.*, 2007).

2.2.2. Radiobiological analysis. Molecular and cellular mechanisms involved in PAT-Plat have now been identified (Corde *et al.*, 2003; Biston *et al.*, 2004). Radiochemotherapy with cisplatin is a representative example of the interplay between different repair pathways evoked in the *Introduction* (Table 1). Indeed, DNA double-strand breaks (DSBs) produced by X-rays are generally repaired by the NHEJ process that is initiated by the translocation of a protein called Ku up to the site of the breaks. Cisplatin molecules preferentially target the DNA of proliferating cells and DNA adducts that are generally repaired by a recombination-like repair process. However, the presence of cisplatin on DNA prevents the Ku translocation and significantly inhibits NHEJ. Consequently, association between ionizing radiation and cisplatin results in irreparable DSBs, as long as the concentration of DNA adducts is sufficient and as long as radiation and cisplatin are used concomitantly (Corde *et al.*, 2003). Interestingly, in the particular case of PAT-Plat, the photoactivation of platinum atoms of cisplatin molecules bound to DNA consists of the production of additional DSBs whose repair is naturally inhibited since they are produced in the close vicinity of DNA adducts that block NHEJ. As a result, the excess of irreparable DSBs contributes to increase the therapeutic index of targeted tumours. Unlike CT therapy with ICAs, since platinated agents bind preferentially the DNA of proliferating tumours, the effects to surrounding tissues are expected to be limited (Corde *et al.*, 2003; Biston *et al.*, 2004).

However, extensive *in vitro* and *in vivo* experiments are still necessary to propose a molecular model of the mechanisms involved in the PAT-Plat approach in order to secure its clinical transfer. Although the PAT-Plat data are encouraging, a number of important questions have to be asked, notably the choice of the energy, the molecular specificities of the technique and the appropriateness of platinated agents in anti-glioma treatments.

(i) Choice of photoactivation energy. PAT-Plat experiments were performed at the platinum *K*-edge and not at the energy

corresponding to the maximal relative X-ray energy absorption of platinum atoms in water (maximum around 40 keV). *In vitro* experiments under PAT-Plat conditions confirmed that the maximal production of DSBs is observed at the *K*-edge and not at 40 keV. A possible explanation is that the *K*-edge energy is the optimized energy of photoactivation when the photoactivable agent is localized inside cell nuclei. Conversely, the maximal relative X-ray energy absorption of the high-Z element in water would be the optimized energy of photoactivation when the photoactivable agent is surrounded by water outside the cell. Further radiochemical investigations are obviously required to consolidate such a hypothesis and would be useful for a general understanding of the biological effects of photoactivation.

(ii) Molecular specificities of the PAT-Plat technique. As mentioned above, the NHEJ pathway, the major DSB repair in mammals, is sterically inhibited by the presence of cisplatin. However, recombination pathways can compensate the NHEJ impairment. In particular, when some proteins essential for recombination, such as BRCA1 or BRCA2, are functional, tumours may be resistant to PAT-Plat (Zhang & Powell, 2005). A careful consideration of the genetic status of the tumour is therefore needed.

(iii) Appropriateness of platinated agents. Anti-glioma treatments with adjuvant cisplatin injection are still a failure to date (Behin *et al.*, 2003). However, it must be stressed that most cisplatin–radiation combinations were performed with intravenous cisplatin administration whereas cisplatin was reported to be more efficient when injected locally (Sheleg *et al.*, 2002; Fehlaue *et al.*, 2005; Biston *et al.*, 2004). Our conclusions therefore encourage the development of PAT-Plat with intracranial injection of a platinated agent (Sheleg *et al.*, 2002; Fehlaue *et al.*, 2005).

3. Applications of micrometric synchrotron X-rays: the MRT approach

3.1. Main principles and first results

In the two previous sections, the CT therapy and PAT-Plat approaches were presented as direct applications of monochromatic synchrotron X-rays. As evoked in the *Introduction*, the high fluence of synchrotrons also makes possible the production of polychromatic micrometric beams allowing a very precise tumour targeting with an extremely high dose rate: grid radiotherapy (Slatkin *et al.*, 1992; Laissue *et al.*, 1998). The accumulation of interlaced micrometric X-ray beams during a single session enables the deliverance of very high radiation doses up to thousands of Grays in a few milliseconds. Grid radiotherapy and its application to brain tumours are mainly based on three observations or postulates: (i) threshold doses for complications of radiotherapy increase as the irradiated volume of tissue is made smaller (Withers *et al.*, 1988); (ii) normal rat brain tissue displays an unusual radioresistance and therefore permits the application of very high doses into the tumour (Dilmanian *et al.*, 2006); (iii) an excess of dose into the tumour should result in destruction of

the tumour vasculature while lower doses in surrounding tissues should insure a significant repopulation of normal cells (Laissue *et al.*, 1998; Dilmanian *et al.*, 2002, 2006; Smilowitz *et al.*, 2006) (Fig. 1).

The physical properties of synchrotron X-rays permitted the feasibility of MRT by providing arrays of parallel thin planar microslices. Furthermore, the use of X-rays in the tens to hundreds of keV range enables higher energy absorption in the tissues. Among the medical applications of synchrotron radiation presented here, MRT studies represent the largest amount of data. The MRT technique was initiated at the National Synchrotron Light Source at Brookhaven National Laboratory (Slatkin *et al.*, 1992, 1995) and was developed at the ESRF. MRT was essentially applied to rat brains (Laissue *et al.*, 1998; Dilmanian *et al.*, 2002), mice (Miura *et al.*, 2006) and also duck embryos (Dilmanian *et al.*, 2001) and piglets (Laissue *et al.*, 2007). MRT irradiation sessions are generally based on a single fraction of radiation dose delivered either unidirectionally or bidirectionally (co- or cross-planar). The total dose (120–1335 Gy) and the geometry parameters differ depending on the experiments and the research groups. The width of the beam varies between 25 and 90 μm and the space between each beam varies between 50 and 300 μm . Two complementary approaches can be considered in the published papers about MRT: those that deal with the regeneration of microvessels after MRT sessions and those that deal with the survival of MRT-treated animals.

With regard to physiological studies of MRT, a dose of thousands of Grays undoubtedly leads to the loss of neuronal and astocytic cell nuclei inside the peak tracks. Physio-pathology and histology observations indicate that rat skin can tolerate a 23-fold higher dose delivered in MRT sessions than in broad beams even. However, some peritumoral necrosis and hypervascularity phenomena were clearly reported in the peritumoral zone even if they do not necessarily affect the final survival outcome (Zhong *et al.*, 2003). For duck embryos, 160 Gy MRT appeared to be equivalent to an 18 Gy broad beam (Dilmanian *et al.*, 2001). With regard to piglets, the animals have been irradiated with microbeams up to 600 Gy and no late tissue effect has been reported (Laissue *et al.*, 2007). There is still no available data about the potential tissue effects of the MRT technique to human cells. Hence, obvious care must be taken in the extrapolation of these observations in animals to humans. In addition, no molecular and stress signaling data about MRT effects are yet available. However, a more recent report aimed to investigate the early effects of 312 or 1000 Gy MRT upon the integrity of the normal microvasculature in mice. Interestingly, intravital dyes remained in the vessels after irradiation from 12 h until three months following 1000 Gy and no extravascular diffusion was observed (Serduc *et al.*, 2006). This radioresistance phenomenon was not observed in 9L glioma microvessels, consolidating therefore the differential effect expected between normal and tumour brain tissues in rodents (Dilmanian *et al.*, 2003). A number of questions remain unsolved however, notably with regard to the death pathways that MRT would specifically induce in glial tissue and/or in vasculature. The use

of innovative technologies such as two-photon microscopy will undoubtedly help in progressing (Serduc *et al.*, 2006).

With regard to the survival of animals treated to MRT, the great majority of authors have used 9L glioma as a model, probably for practical reasons (high proliferation rate, availability of the cell lines in the laboratory *etc.*). The highest median survival time values provided to date by MRT is 171 days for rats (Smilowitz *et al.*, 2006) and about 40 days for mice (Miura *et al.*, 2006). Recently, Dilmanian *et al.* (2006) summarized the requirement of the geometry MRT parameters to obtain optimized survival data as follows: (i) for a given dose the beam thickness should not exceed a certain width; (ii) for a given thickness the valley dose should be minimized; (iii) the peak dose should be lower than the dose that kills neurons in the direct path of the microbeam. Survival data will be reviewed in the next chapter.

3.2. Radiobiological features

From theoretical simulations, it appears that the dose delivered in the valleys may represent 1–10% of the dose (Dilmanian *et al.*, 2006; Siegbahn *et al.*, 2006). For 500–1000 Gy delivered into the peak, these data suggest that a minimum of 5–10 Gy may be delivered in tissues between two peaks and in close vicinity of the tumour. MRT has been essentially applied to rat 9L glioma and modeled from rodent observations. Mammalian and notably rodent cells have long been shown to be much more radioresistant than human cells (Bencokova *et al.*, 2007). The 9L model is one of the most radioresistant rodent cell lines and its clonogenic survival following X-ray exposure is at the upper limit of radioresistance observed in human cells (Bencokova *et al.*, 2007). As an example, about 20% and less than 1% cell survival is expected after 5 and 10 Gy X-rays (200 kV), respectively, with the same model. The cell survivals after the same doses are about 5% and negligible for human radioresistant cells, respectively (Chavaudra *et al.*, 2004; Bencokova *et al.*, 2007; Joubert *et al.*, 2007). Further, it is noteworthy that cellular repopulation is not observed after 6 Gy even for the most radioresistant human tumour cells whereas the cell cycle is not totally arrested with 9L cells (Bencokova *et al.*, 2007). Hence, even if the dose delivered in the valley may have no impact in rodents, again care must be taken before extrapolating rodent data to humans. Hence, the choice of the total dose inside the tumour will be one of the most important challenges of the clinical transfer of MRT to humans.

This last paragraph raises another radiobiological feature that must also be considered for MRT on any biological scale: what happens in the surrounding normal human tissues after the deliverance of such high radiation doses? In the past 50 years a considerable amount of data have suggested the existence of significant biological effects in cells that are not directly hit by radiation tracks. Even if these effects do not necessarily proceed from a single cause and despite the fact that their molecular bases remain to be elucidated, radiobiologists describe them under the general term of radiation-induced bystander effects (RIBE) (Mothersill & Seymour,

2004*a,b*). The most relevant models of RIBEs mainly involve calcium ions. The cell can be considered as an electrostatic dipole. Ionizing radiation leads to a depolarization of the cell membrane and a brief release of calcium ions. Such potential oxidative stress can diffuse through a liquid medium and concern cells that were not targeted initially by radiation (Ponnaiya *et al.*, 2004; Yang *et al.*, 2005). This phenomenon occurs also *in vivo* in tissues and is described as abscopal effects (Charles, 2001). RIBEs favour the extension of dose effects to tissue up to tens of micrometres *in vitro* and up to millimetres *in vivo* and correspond to the equivalent of 10% of the initial dose (Mothersill & Seymour, 2004*a,b*). It is still too early to conclude that RIBEs may be a source of additional stress for normal tissues in MRT modality but preliminary reports indicate that significant RIBE effects (as DSB formation and micronuclei) are clearly observed in human fibroblasts after an MRT treatment (dose, 10 Gy; width, 100 μm ; space between tracks, 500 μm). These findings suggest that RIBE effects after MRT may impact significantly upon human cell viability (Joubert *et al.*, 2007). Only one report dealing with MRT raises the problem of the bystander effect (Dilmanian *et al.*, 2007). However, this study does not include molecular and stress signaling analysis of RIBEs and authors interpret the repopulation of mammalian cells surrounding those inside tracks as a beneficial bystander effect throughout the effect of very low doses (Dilmanian *et al.*, 2007). While the beneficial effect of very low doses is still a source of disagreement between authors and must be carefully considered (Krause *et al.*, 2005; Joiner *et al.*, 2001), no quantification of DNA damage in the bystander cells during MRT treatment has been performed yet. Lastly, the impact of bystander effects is expected to diminish gradually as far as the distance from the targeted cells increases. Consequently, even if beneficial bystander effects may be observed in bystander cells far from the peak, the question of their toxicity in normal cells in the close vicinity of the targeted tumour tissue remains unsolved. Hence, further biochemical investigations and data on human cells are needed to better understand the bystander effects potentially induced by microbeams and particularly whether bystander effects can explain the necrosis and hypervascularity phenomena observed in the peritumoral zones during some MRT treatments (Zhong *et al.*, 2003).

4. How to evaluate anti-cancer strategies involving synchrotron X-rays and perform relevant comparisons

4.1. Difficulties specific to gliomas

To date, almost all the preclinical assays involving synchrotron X-rays have been performed on gliomas inoculated to rats. Indeed, it was natural that innovative anti-cancer strategies aim to target the most radioresistant tumour types. Deriving from glial, astrocyte or dendrocyte cells, gliomas are the most frequent tumours of the central nervous system. Unfortunately, most gliomas are refractory to standard treatments (Behin *et al.*, 2003). The median survival for patients bearing grade IV gliomas (glioblastomas) does not exceed one

year even after both aggressive surgery and radiotherapy treatment. Chemotherapy alone also leads to discouraging results. The median survival after radiotherapy associated with adjuvant chemotherapy does not exceed one year as well. A standard of 60 Gy delivered in 30 fractions during six weeks remains the best modality against gliomas (Behin *et al.*, 2003). Finally, human gliomas appear to be very heterogeneous which makes the prediction of clinical efficiency from *in vitro* clonogenic survival data very difficult (Taghian *et al.*, 1993). Hence, care must be taken for the choice of cellular glioma models, whether from rodents or humans. A recent study showed that 9L, F98 and C6, three of the most extensively used rat glioma models, elicit different molecular and cellular responses to radiation and cisplatin. Notably, some differences have been attributed to impairments of the BRCA1 protein: 9L appeared BRCA1-positive whereas F98 and C6 elicit a truncated or cytoplasmic form of BRCA1, respectively (Bencokova *et al.*, 2007). The genetic status of the p16 pathway, downstream to the BRCA1 function, has been shown to be different in these three models as well (Schlegel *et al.*, 1999). In addition to these functional and genetic specificities, these three models also elicit different physiological characteristics such as shape, proliferation rate and immunogenic responses, raising the problem of the extrapolation of rodent models to human. Hence, like any other innovative anti-glioma approach, the molecular and cellular response to human glioma cell lines has to be documented to verify hypotheses established from rodent data.

4.2. Endpoints required for comparisons

In the framework of the considerable amount of data accumulated these past few years, it is legitimate to ask whether the three medical applications of synchrotron X-rays described above are equally efficient against gliomas. An objective comparison of CT therapy, PAT-Plat and MRT requires the choice of relevant endpoints to allow quantitative comparisons. Among the plethora of data, the survival of rats bearing glioma appeared to be the best compromise since rats are the only animal model used in common with CT therapy, PAT-Plat and MRT. Unfortunately, different cellular models of rat gliomas have been used. The choice of rodent glioma models is notably mainly motivated by the existence of previous data in the laboratory, their proliferation capacity in culture and/or in animals and their non-immunogenic properties, rather than specific molecular features or genetic status (Bencokova *et al.*, 2007). All of the published MRT studies with rats dealt with the 9L model whereas CT therapy and PAT-Plat were applied to F98 (Table 2, and references herein).

With regard to the choice of endpoints, the percentage of survival rats appears to be a natural parameter. However, the number of treated rats differs roughly from one report to another and should also be considered in intercomparisons. Further, the confidence zone of the survival time of untreated rats that may vary from one author to another should also be considered to better evaluate the excess of survival provided by the treatment. Lastly, comparisons of the different rat

Table 2

Best results of preclinical trials using synchrotron radiation in rats bearing gliomas.

i.p. = intraperitoneally; i.v. = intravenously; i.c.r. = intracranially. Values shown in bold are the best protracted survivals of treatment modality.

Tumour model	Treatment and irradiation modality	Median survival time (days) (number of rats) [Surface under curve]†	Rats surviving at 50, 100, 150, 200 days post-treatment (%)	Increased life span of MeST (%)	Reference
Microbeam radiation therapy (MRT)					
9L glioma in Fisher rats	Untreated controls	25 (9)	–	–	Laissue <i>et al.</i> (1998)
	625 Gy unidirectionally	45 (11)	35, 35, 35, 35	80	
	625 Gy bidirectionally	115 (14)	100, 55, 50, 50	360	
9L glioma in Fisher rats	Untreated controls	19 (17)	–	–	Dilmanian <i>et al.</i> (2002)
	150 Gy, 50 µm beam spacing	98 (5)	60, 60, 40, 40	415	
	250 Gy, 75 µm beam spacing	171 (5) [145]	100, 60, 60, 40	800	
9L glioma in Fisher rats	500 Gy, 100 µm beam spacing	170 (3)	65, 65, 65, 32	794	Smilowitz <i>et al.</i> (2006)
	Untreated controls	9 (14)	–	–	
	625 Gy unidirectionally	25 (25)	40, 20, 20, 20	170	
	625 Gy unidirectionally + IMPR	25 (14)	24, 20, 20, 20	170	
9L glioma in Fisher rats	625 Gy unidirectionally + GMIMPR	32 (23)	47, 42, 42, 42	255	
Boron neutron capture therapy (BNCT)					
9L glioma in Fisher rats	Untreated controls	22 (18)	–	–	Coderre <i>et al.</i> (1994)
	22.5 Gy X-rays controls	35 (55)	27, 20, 20, 20	59	
	7.5 MW-min + boronophenilalanine + mannitol i.p.	130 (12) [142.5]	100, 60, 50, 50	491	
Photoactivation of iodinated contrast agents (CT therapy)					
F98 glioma in Fisher rats	Untreated controls	12 (6)	–	–	Adam <i>et al.</i> (2003)
	10 Gy (50 keV)	15 (6)	0, 0, 0, 0	20	
	10 Gy (50 keV) + Iomeron	17 (6)	0, 0, 0, 0	44	
F98 glioma in Fisher rats	Untreated	26 (9)	–	–	Adam <i>et al.</i> (2006)
	15 Gy (50 keV)	46 (15)	40, 0, 0, 0	77	
	15 Gy (50 keV) + i.v. Iomeron + mannitol	54 (10)	60, 0, 0, 0	108	
	15 Gy (50 keV) + i.c. Iomeron + mannitol	71 (9) [92.5]	90, 0, 0, 0	173	
	25 Gy (50 keV)	145 (9)	90, 90, 40, 10	458	
	25 Gy (50 keV) + i.v. Iomeron + mannitol	55 (9)	60, 0, 0, 0	113	
	25 Gy (50 keV) + i.c. Iomeron + mannitol	45 (11)	35, 0, 0, 0	73	
Photoactivation of platinated compounds (PAT-Plat)					
F98 glioma in Fisher rats	Untreated	26 (12)	–	–	Biston <i>et al.</i> (2004)
	15 Gy (78 keV)	48 (10)	50, 0, 0, 0	85	
	i.c.r. 3 µg cisplatinium	37 (10)	10, 0, 0, 0	42	
	15 Gy (78 keV) + i.c.r. 3 µg cisplatinium exp1	206 (18) [153.7]	90, 67, 65, 65	694	
	15 Gy (78 keV) + i.c.r. 3 µg cisplatinium exp2	110 (10) [118.7]	65, 60, 40, 40	323	
F98 glioma in Fisher rats	Untreated	26 (20)	–	–	Biston <i>et al.</i> (2007)
	15 Gy (78 keV)	34 (5)	50, 0, 0, 0	31	
	i.c.r. 3 µg cisplatinium	41 (15)	30, 0, 0, 0	58	
	i.c.r. 40 µg carboplatinium	58 (9)	50, 10, 10, 10	123	
	15 Gy (78 keV) + i.c.r. 3 µg cisplatinium	95 (25)	85, 45, 40, 37	265	
	15 Gy (78 keV) + i.c.r. 40 µg carboplatinium	111 (17)	70, 50, 40, 20	326	
Boron neutron capture therapy (BNCT)					
F98 glioma in Fisher rats	Untreated controls	25 (10)	–	–	Barth <i>et al.</i> (2000)
	BNCT (boronophenilalanine sodium borocaptate + mannitol i.c.)	72 (20) [111.2]	85, 50, 25, 25	483	

† Calculated in days up to 200 days post-treatment.

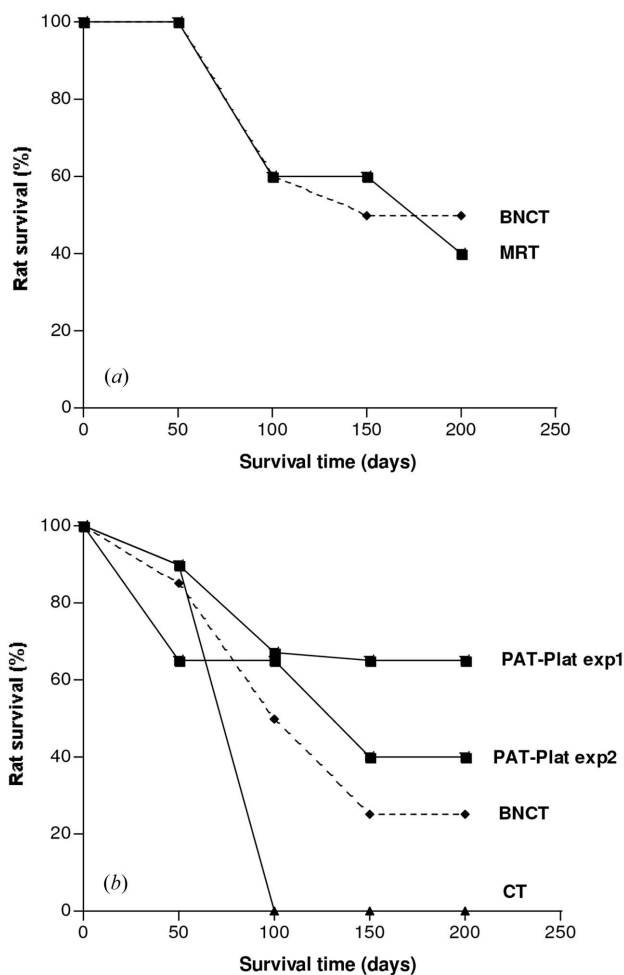


Figure 2
The best results obtained using anti-cancer synchrotron radiation treatments. Quantitative illustration of the highest percentages of survival of rats bearing the 9L (a) and F98 (b) glioma treated to the indicated synchrotron modalities. The values shown here are those presented in bold characters in Table 2. A correlation exists between the surface under the curves (S) and the MeST values: $S = -192.51 + 153.79 \ln(\text{MeST})$; $r = 0.976$, $p < 0.01$.

survival curves in the literature is made difficult by the unavoidably low number of replicates owing to the availability of synchrotron beamlines. Hence, we endeavoured to use the highest median survival time (MeST), the number of rats and the percentage of rats surviving at 50, 100, 150 and 200 days post-treatment as endpoints to provide an objective quantification of survival data by taking into account the early and delayed effects owing to each modality. As a first step, only the best quantitative results of preclinical assays with rats bearing gliomas treated with synchrotron radiation have been reviewed in CT therapy, PAT-plat and MRT (Table 2, Fig. 2).

4.3. Analysis of survivals of rats treated to MRT

With regard to the MRT preclinical assays, a number of beamline parameters (dose, beam spacing, beam size etc.) make any comparisons difficult. However, with the same 9L glioma model, it appears that it is not necessarily the highest radiation dose applied to the tumour volume that provides the

most protracted rat life span (Table 2, Fig. 2). In fact, the highest MeST was obtained with 250 Gy and 75 μm beam spacing whereas doses up to 625 Gy have already been tested. Boron neutron capture therapy (BNCT), based on preferential energy absorption in boron by neutrons, has been also applied to the 9L model. BNCT therefore represents a good reference for comparison, inasmuch as the MeST value for untreated rats (22 days) obtained using this approach was found to be similar to those obtained with MRT. BNCT showed an impressive MeST of 250 days (the highest MeST obtained with the 9L model) whereas the highest MeST values provided to date by MRT is 171 days with five rats (Table 2, Fig. 2).

4.4. Analysis of survivals of rats treated to CT therapy

Until recently, only two groups have developed the CT therapy with ICAs (Norman *et al.*, 1991; Adam *et al.*, 2003, 2006). With regard to preclinical assays with rats, CT therapy was applied to the F98 model only. Similarly to MRT, it is not necessarily the highest radiation dose applied to the tumour that provides the most protracted rat life span (Table 2, Fig. 1). A representative example is given by Adam *et al.* (2006) who showed that an exposure of 25 Gy alone is more efficient against tumours than when combining with ICAs. The most efficient treatment with ICAs appears to be 15 Gy with ICAs injected into carotid (Adam *et al.*, 2006). BNCT was also applied to the F98 model with a similar MeST of untreated rats (25 days). BNCT-treated rats bearing gliomas showed similar MeST as those treated to CT therapy with ICAs (71 versus 72 days) (Barth *et al.*, 2000), suggesting that either F98 is a model specifically refractory to these both modalities and/or that CT therapy with ICAs does not provide a significant improvement of rat life span (Table 2, Fig. 2).

4.5. Analysis of survivals of rats treated to PAT-Plat

PAT-Plat strategy was also applied to the F98 model (Biston *et al.*, 2004, 2007). With this model the PAT-Plat approach provides much higher MeST values (up to three times higher) than CT therapy and BNCT together, with similar MeST obtained with untreated rats (Table 2, Fig. 1) (Biston *et al.*, 2004). Differences in MeST may have been observed by replacing cisplatin by carboplatin (Biston *et al.*, 2007). Interestingly, unlike CT therapy with ICAs, PAT-Plat studies and MRT are the only medical applications of synchrotron X-rays that elicit non-negligible percentages of rats surviving after 100 days post-treatment (Table 2, Fig. 2).

5. Conclusions

Like any other innovative anti-cancer approaches, the medical applications of synchrotrons reviewed here should consider the following basic points: (i) how can the side effects specifically due to the innovating treatment be evaluated, predicted and prevented? (ii) can data obtained from animal models be extrapolated to humans? (iii) how can quantificated proofs of

the benefit of a given approach compared with the existing modalities be provided?

Furthermore, because of the physical properties specific to synchrotron X-rays, additional points have to be considered; notably, physical events of photoactivation are still undefined (photoelectric effect? Auger effect? *etc.*) and their relative contribution to the final clinical outcome in the three medical applications of synchrotron radiation remains undetermined. A better knowledge of the early physical events following an exposure to synchrotron X-rays would help in determining the optimized energy that provides maximal photoactivation and synergy. For example, such an approach could be pursued by further *in vitro* investigations with iodine by using different monochromatic synchrotron X-ray energies.

The PAT-Plat strategy is a representative example of innovating anti-cancer strategy that endeavours to associate the benefit of both radiation and chemotherapy. However, such association raises the problem of co-toxicities with concomitant induction of different DNA damage types that are repaired by different repair pathways. Hence, pharmacomodulation of DNA repair necessarily implicates a differential tumour targeting depending on genetic status. Platinated agents involved in PAT-Plat target DNA directly and inhibit DNA repair. This is not the case for ICAs that do not cross the cell membrane nor reach DNA. Considering the impact of DNA damage upon cell lethality, this would explain the relative failure of CT therapy and the good results of PAT-Plat (Joubert *et al.*, 2005). The PAT-Plat effect also raises the importance of genetic status that may determine the final clinical outcome of the patients. The use of different models, whether animals or cell lines, would help in detailing the molecular specificities of each modality.

MRT more likely raises the problem of RIBEs and the response to surrounding tissues that may also condition the patient outcome. RIBEs will unavoidably represent a challenge in the future for a novel definition of the radiation dose. The radiation dose acceptable for rodents may provide a differential therapeutic benefit in humans. Furthermore, MRT, based on a precise irradiation set-up (array of micrometric beams), must take into account the breathing movements of patients that may infer onto the target practically irradiated (Table 1). Hence, mainly based on rodent data, the MRT technique should be tested in human glioma models.

The increasing amount of data involving anti-cancer strategies using synchrotron radiation prompted us to evaluate their potential clinical transfer by carefully considering their radiobiological features. Obviously, extreme care must be taken when considering comparisons of medical applications of synchrotron radiation (Table 1). In addition, the comparisons of rat survival data provided by the different modalities raises unavoidable questions with regard to the statistical analysis. In the 1980s, a similar problem occurred for the comparisons of *in vitro* clonogenic survival curves. The use of the only survival fraction at 2 Gy (SF2), useful for radiotherapists, to reflect all the curves was a subject of hard discussions between scientists, notably when curves cross. Fertil and Malaise proposed to consider not the survival data

at a given dose but rather the surface under the curve that corresponds to the integral of the survival curve. Such a parameter was defined as the mean inactivation dose \bar{D} (dose giving 37% survival) and was shown to reflect the survival curve better than SF2 (Fertil *et al.*, 1984). Hence, we preliminarily examined the surface under the curves shown in Fig. 2 expressed as surviving fraction \times time unit (days). These values are detailed in Table 2. A preliminary analysis indicates that the surface under the curve correlates well with the median survival time but provides a different scale for comparison (see legend to Fig. 2). A systematic evaluation of both MeST and the surface under the curve may help in quantitative comparisons of the survival data.

A number of other potentially photoactivable elements are actually at the origin of molecular and cellular *in vitro* studies. This is notably the case of gadolinium components (De Stasio *et al.*, 2006) that are extensively used in nuclear magnetic resonance imaging. Some preliminary studies are also foreseen with gold nanoparticles (Hainfeld *et al.*, 2004, 2006). Synchrotron radiation appears to be a key tool for increasing the knowledge of radiation-induced phenomena and for developing innovative strategies against cancer. MRT and PAT-Plat approaches appear to be promising strategies against gliomas, notably because they show equivalent or better results than BNCT. However, a systematic screening of repair gene mutations of tumours and a transversal approach integrating molecular, cellular and tissular biological investigations are required to insure the most specific and appropriate anti-cancer treatment to each individual case. The use of synchrotron radiation combined with biologically personalized anti-cancer treatments will be undoubtedly one of the major challenges of the future.

We thank V. Favaudon and A.-M. Charvet for fruitful discussions. ZB is a PhD fellowship of Roche-France. This work was also supported by the Association Pour la Recherche sur l'Ataxie-Telangiectasie (APRAT), Association pour la Recherche contre le Cancer (ARC), the Ligue contre le Cancer (Comité de Savoie), the Electricité de France (Comité de Radioprotection), the TOXNUC and the ETOILE Project (Région Rhône-Alpes and Lyon University).

References

- Adam, J. F., Elleaume, H., Joubert, A., Biston, M. C., Charvet, A. M., Balosso, J., Le Bas, J. F. & Esteve, F. (2003). *Int. J. Radiat. Oncol. Biol. Phys.* **57**, 1413–1426.
- Adam, J. F., Joubert, A., Biston, M. C., Charvet, A. M., Peoc'h, M., Le Bas, J. F., Balosso, J., Esteve, F. & Elleaume, H. (2006). *Int. J. Radiat. Oncol. Biol. Phys.* **64**, 603–611.
- Adams, F. H., Norman, A., Mello, R. S. & Bass, D. (1977). *Radiology*, **124**, 823–826.
- Barth, R. F., Yang, W., Rotaru, J. H., Moeschberger, M. L., Boesel, C. P., Soloway, A. H., Joel, D. D., Nawrocky, M. M., Ono, K. & Goodman, J. H. (2000). *Int. J. Radiat. Oncol. Biol. Phys.* **47**, 209–218.
- Behin, A., Hoang-Xuan, K., Carpentier, A. F. & Delattre, J. Y. (2003). *Lancet*, **361**, 323–331.

- Bencokova, Z., Pauron, L., Devic, C., Joubert, A., Gastaldo, J., Massart, C., Balosso, J. & Foray, N. (2007). *J. Neurooncol.* Accepted.
- Biston, M. C., Joubert, A., Adam, J. F., Elleaume, H., Bohic, S., Charvet, A. M., Esteve, F., Foray, N. & Balosso, J. (2004). *Cancer Res.* **64**, 2317–2323.
- Biston, M., Joubert, A., Elleaume, H., Charvet, A., Estève, F., Balosso, J. & Foray, N. (2007). Submitted.
- Boudou, C., Balosso, J., Esteve, F. & Elleaume, H. (2005). *Phys. Med. Biol.* **50**, 4841–4851.
- Cepeda, V., Fuertes, M. A., Castilla, J., Alonso, C., Quevedo, C. & Perez, J. M. (2007). *Anticancer Agents Med. Chem.* **7**, 3–18.
- Charles, M. (2001). *J. Radiol. Prot.* **21**, 83–86.
- Chavaudra, N., Bourhis, J. & Foray, N. (2004). *Radiother. Oncol.* **73**, 373–382.
- Coderre, J. A., Button, T. M., Micca, P. L., Fisher, C. D., Nawrocky, M. M. & Liu, H. B. (1994). *Int. J. Radiat. Oncol. Biol. Phys.* **30**, 643–652.
- Corde, S., Balosso, J., Elleaume, H., Renier, M., Joubert, A., Biston, M. C., Adam, J. F., Charvet, A. M., Brochard, T., Le Bas, J. F., Esteve, F. & Foray, N. (2003). *Cancer Res.* **63**, 3221–3227.
- Corde, S., Joubert, A., Adam, J. F., Charvet, A. M., Le Bas, J. F., Esteve, F., Elleaume, H. & Balosso, J. (2004). *Br. J. Cancer*, **91**, 544–551.
- De Stasio, G., Rajesh, D., Ford, J. M., Daniels, M. J., Erhardt, R. J., Frazer, B. H., Tyliczszak, T., Gilles, M. K., Conhaim, R. L., Howard, S. P., Fowler, J. F., Esteve, F. & Mehta, M. P. (2006). *Clin. Cancer Res.* **12**, 206–213.
- Dilmanian, F. A. *et al.* (2001). *Cell Mol. Biol.* **47**, 485–493.
- Dilmanian, F. A. *et al.* (2002). *Neurooncology*, **4**, 26–38.
- Dilmanian, F. A. *et al.* (2005). *Nucl. Instrum. Methods Phys. Res. A*, **548**, 30–37.
- Dilmanian, F. A., Hainfeld, J. F. & Krause, C. A. (2003). *NSLS Activity Report 2002*. National Synchrotron Light Source, New York, USA.
- Dilmanian, F. A., Qu, Y., Feinendegen, L. E., Pena, L. A., Bacarian, T., Henn, F. A., Kalef-Ezra, J., Liu, S., Zhong, Z. & McDonald, J. W. (2007). *Exp. Hematol.* **35**, 69–77.
- Dilmanian, F. A., Zhong, Z., Bacarian, T., Benveniste, H., Romanelli, P., Wang, R., Welwart, J., Yuasa, T., Rosen, E. M. & Anshel, D. J. (2006). *Proc. Natl. Acad. Sci. USA*, **103**, 9709–9714.
- Dudas, A. & Chovanec, M. (2004). *Mutat. Res.* **566**, 131–167.
- Fairchild, R. G. (1987). *Int. J. Radiat. Oncol. Biol. Phys.* **13**, 1262–1263.
- Fairchild, R. G., Brill, A. B. & Ettinger, K. V. (1982). *Invest. Radiol.* **17**, 407–416.
- Fehlauer, F., Muench, M., Rades, D., Stalpers, L. J., Leenstra, S., van der Valk, P., Slotman, B., Smid, E. J. & Sminia, P. (2005). *J. Cancer Res. Clin. Oncol.* **131**, 723–732.
- Fertil, B., Dertinger, H., Courdi, A. & Malaize, E. P. (1984). *Radiat. Res.* **99**, 73–84.
- Goodhead, D. T., Thacker, J. & Cox, R. (1981). *Phys. Med. Biol.* **26**, 1115–1127.
- Hainfeld, J. F., Slatkin, D. N., Focella, T. M. & Smilowitz, H. M. (2006). *Br. J. Radiol.* **79**, 248–253.
- Hainfeld, J. F., Slatkin, D. N. & Smilowitz, H. M. (2004). *Phys. Med. Biol.* **49**, N309–N315.
- Iwamoto, K. S., Cochran, S. T., Winter, J., Holburt, E., Higashida, R. T. & Norman, A. (1987). *Radiother. Oncol.* **8**, 161–170.
- Iwamoto, K. S., Norman, A., Freshwater, D. B., Ingram, M. & Skillen, R. G. (1993). *Radiother. Oncol.* **26**, 76–78.
- Jeggio, P. A. & Loblrich, M. (2006). *DNA Repair (Amst.)* **5**, 1192–1198.
- Joiner, M. C., Marples, B., Lambin, P., Short, S. C. & Turesson, I. (2001). *Int. J. Radiat. Oncol. Biol. Phys.* **49**, 379–389.
- Joubert, A., Biston, M. C., Boudou, C., Ravanat, J. L., Brochard, T., Charvet, A. M., Esteve, F., Balosso, J. & Foray, N. (2005). *Int. J. Radiat. Oncol. Biol. Phys.* **62**, 1486–1496.
- Joubert, A. & Foray, N. (2006). In *New Research on DNA Repair*, edited by B. R. Landseer, ch. 10. Hauppauge: Nova Science.
- Joubert, A., Zimmerman, K. M., Bencokova, Z., Gastaldo, J., Chavaudra, N., Favaudon, V., Arlett, C. F. & Foray, N. (2007). *Int. J. Radiat. Biol.* In the press.
- Kassis, A. I. & Adelstein, S. J. (1996). *J. Nucl. Med.* **37**, 10S–12S.
- Khanna, K. K. & Jackson, S. P. (2001). *Nat. Genet.* **27**, 247–254.
- Krause, M., Wohlfarth, J., Georgi, B., Pimentel, N., Dorner, D., Zips, D., Eicheler, W., Hessel, F., Short, S. C., Joiner, M. C. & Baumann, M. (2005). *Int. J. Radiat. Biol.* **81**, 751–758.
- Laissue, J. A., Blattman, H., Wagner, H. P., Grotzer, M. A. & Slatkin, D. N. (2007). *Dev. Med. Child Neurol.* **49**, 577–581.
- Laissue, J. A., Geiser, G., Spanne, P. O., Dilmanian, F. A., Gebbers, J. O., Geiser, M., Wu, X. Y., Makar, M. S., Micca, P. L., Nawrocky, M. M., Joel, D. D. & Slatkin, D. N. (1998). *Int. J. Cancer*, **78**, 654–660.
- Laster, B. H., Thomlinson, W. C. & Fairchild, R. G. (1993). *Radiat. Res.* **133**, 219–224.
- Mitchell, J. B., Russo, A., Cook, J. A., Straus, K. L. & Glatstein, E. (1989). *Int. J. Radiat. Biol.* **56**, 827–836.
- Miura, M., Blattmann, H., Brauer-Krisch, E., Bravin, A., Hanson, A. L., Nawrocky, M. M., Micca, P. L., Slatkin, D. N. & Laissue, J. A. (2006). *Br. J. Radiol.* **79**, 71–75.
- Mothersill, C. & Seymour, C. (2004a). *Mutat. Res.* **568**, 121–128.
- Mothersill, C. & Seymour, C. B. (2004b). *Nat. Rev. Cancer*, **4**, 158–164.
- Norman, A., Adams, F. H. & Riley, R. F. (1978). *Radiology*, **129**, 199–203.
- Norman, A., Cochran, S. T. & Sayre, J. W. (2001). *Radiat. Res.* **155**, 740–743.
- Norman, A., Ingram, M., Skillen, R. G., Freshwater, D. B., Iwamoto, K. S. & Solberg, T. (1997). *Radiat. Oncol. Investig.* **5**, 8–14.
- Norman, A., Iwamoto, K. S. & Cochran, S. T. (1991). *Invest. Radiol.* **26**, S120–S121; discussion S125–128.
- Ponnaiya, B., Jenkins-Baker, G., Brenner, D. J., Hall, E. J., Randers-Pehrson, G. & Geard, C. R. (2004). *Radiat. Res.* **162**, 426–432.
- Rabik, C. A. & Dolan, M. E. (2007). *Cancer Treat. Rev.* **33**, 9–23.
- Rose, J. H., Norman, A., Ingram, M., Aoki, C., Solberg, T. & Mesa, A. (1999). *Int. J. Radiat. Oncol. Biol. Phys.* **45**, 1127–1132.
- Rothkamm, K. & Loblrich, M. (2003). *Proc. Natl. Acad. Sci. USA*, **100**, 5057–5062.
- Santos Mello, R., Callisen, H., Winter, J., Kagan, A. R. & Norman, A. (1983). *Med. Phys.* **10**, 75–78.
- Schlegel, J., Piontek, G., Kersting, M., Schuermann, M., Kappler, R., Scherthan, H., Weghorst, C., Buzard, G. & Mennel, H. (1999). *Pathobiology*, **67**, 202–206.
- Serduc, R., Verant, P., Vial, J. C., Farion, R., Rocas, L., Remy, C., Fadlallah, T., Brauer, E., Bravin, A., Laissue, J., Blattmann, H. & van der Sanden, B. (2006). *Int. J. Radiat. Oncol. Biol. Phys.* **64**, 1519–1527.
- Sheleg, S. V., Korotkevich, E. A., Zhavrid, E. A., Muravskaya, G. V., Smeyanovich, A. F., Shanko, Y. G., Yurkshtovich, T. L., Bychkovsky, P. B. & Belyaev, S. A. (2002). *J. Neurooncol.* **60**, 53–59.
- Siegbahn, E. A., Stepanek, J., Brauer-Krisch, E. & Bravin, A. (2006). *Med. Phys.* **33**, 3248–3259.
- Slatkin, D. N., Spanne, P., Dilmanian, F. A., Gebbers, J. O. & Laissue, J. A. (1995). *Proc. Natl. Acad. Sci. USA*, **92**, 8783–8787.
- Slatkin, D. N., Spanne, P., Dilmanian, F. A. & Sandborg, M. (1992). *Med. Phys.* **19**, 1395–1400.
- Smilowitz, H. M., Blattmann, H., Brauer-Krisch, E., Bravin, A., Di Michiel, M., Gebbers, J. O., Hanson, A. L., Lyubimova, N., Slatkin, D. N., Stepanek, J. & Laissue, J. A. (2006). *J. Neurooncol.* **78**, 135–143.
- Steel, G. G. (2002). *Basic Clinical Radiobiology*, 3rd ed. London: Arnold.
- Taghian, A., Ramsay, J., Allalunis-Turner, J., Budach, W., Gioioso, D., Pardo, F., Okunieff, P., Bleehen, N., Urtasun, R. & Suit, H. (1993). *Int. J. Radiat. Oncol. Biol. Phys.* **25**, 243–249.

Turchi, J. J., Patrick, S. M. & Henkels, K. M. (1997). *Biochemistry*, **36**, 7586–7593.

Withers, H. R., Taylor, J. M. & Maciejewski, B. (1988). *Int. J. Radiat. Oncol. Biol. Phys.* **14**, 751–759.

Yang, H., Asaad, N. & Held, K. D. (2005). *Oncogene*, **24**, 2096–2103.

Zhang, J. & Powell, S. N. (2005). *Mol. Cancer Res.* **3**, 531–539.

Zhong, N., Morris, G. M., Bacarian, T., Rosen, E. M. & Dilmanian, F. A. (2003). *Radiat Res.* **160**, 133–142.